Basalt Fibers as composite material for structural elements

Conference Paper · April 2017

CITATION
1

READS
847

2 authors:

Eyþór Rafn Þórhallsson
Reykjavik University
50 PUBLICATIONS **76** CITATIONS
SEE PROFILE

Jónas Þór Snæbjörnsson
Reykjavik University
105 PUBLICATIONS **330** CITATIONS
SEE PROFILE

Basalt Fibers as composite material for structural elements

Eythór Rafn Thórhallsson[1], Jonas Thór Snaebjörnsson[2]

Introduction

Basalt fibre reinforced polymer (BFRP) is an interesting structural material especially in combination with concrete. For instance when designing against thermal shrinkage as in slab on grade, basalt rebars have an advantage in that the thermal expansion coefficient is very close to the thermal shrinkage coefficient of concrete (Williams, 2015).

In an enviromental study of concrete BFRP beams carried out by Wiik, Thorhallsson and Azrague, (2017) one of the core finding was that both BFRP tendons and reinforcement steel bar have similar emission factors: 2,6 and 2,34 kgCO2eq/kg respectively. However, since BFRP has a lower specific weight than steel, and is three times lighter, the overall embodied emissions are much lower in the BFRP reinforced concrete beams. This is because less material (per kg) is required to perform the same function.

During recent years, the structural and composite laboratory at Reykjavik University (SEL) has performed novel experimental and analytical research using continuous basalt fibers as a structural material in composite timber and concrete structures. (Thorhallsson et. al. 2011, 2012, 2013a, 2013b, 2013c, 2014a, 2014b, 2015, 2016a, 2016b), (Johannesson et. al. 2017). The paper will give an overview of these experiments and draw some general conclusions based on the experience accumulated.

The experimental programs to date, involves the following specimens:

- Bending test of prestressed basalt fiber reinforced concrete beams.
- Monitoring of pre-tensioned BFRP bars to estimate loss of prestress.
- Thin concrete panels with basalt fiber mats as tension reinforcement.
- Comparative testing of rectangular steel reinforced concrete columns with and without BFRP wrapping for strengthening.
- Glulam beams strengthened by gluing one-directional basalt mats to the bottom (tension) lamella.
- Concrete beams with BFRP sheets bonded with mortar on the tension side.
- Concrete beams with BFRP mats glued on their sides to improve shear strength behaviour.
- Composite plate specimens produced using basalt fiber mats in polyester resin and tested for tension, compression and shear forces using a standard ASTM test.

In nearly all cases, the experimental results were compared with analytical and/or numerical models. In the following sections a few of the experimental programs listed above are described and the key results summarized.

Prestressed basalt rods for reinforcing concrete beams

Nine beams were prestressed using two 10 mm in diameter BFRP tendons each, delivered by Magma Tech Ireland with the trademark RockBar. The tensile strength of the rods are 1000+ MPa. Each tendon was prestressed to approx. 50% of its ultimate strength. The concrete strength was determined as the mean concrete strength of 3 tests on concrete cylinders carried out 28 days after concrete casting.
The experimental setup and the geometric dimensions of the beam are illustrated in Figure 1. Table 1 provides information about beam size and the total length to the point at which the force ($F/2$) is applied. The prestressing force, P, is listed in column 5 of Table 1. All the tested beams had the same equivalent amount of internal bounded reinforcement and a cross-sectional area A_f = 156 [mm^2]. The bending ratio for all the beams was ρ*= 0,0052.* The maximum value of the shear force ($F/2$), measured in a given test before fracture of concrete, is referred to as V_{exp} in Table 1*.* $M_{at\ failure}$ is the maximum bending moment in

[1] Reykjavik University, Menntavegi 1, Reykjavík,Iceland, eythor@ru.is
[2] Reykjavik University, Menntavegi 1, Reykjavík,Iceland, jonasthor@ru.is

the beam mid-span calculated by multiplying $V_{exp.}$ (factored) by *a*. $V_{craking}$ is the shear force at which macro cracking is initiated (in the four-point bending test). Deflections (Δ [mm]) corresponding to failure load for each beam are listed in Table 1, in the second last column to the right. (Thorhallsson and Snaebjornsson, 2016a)

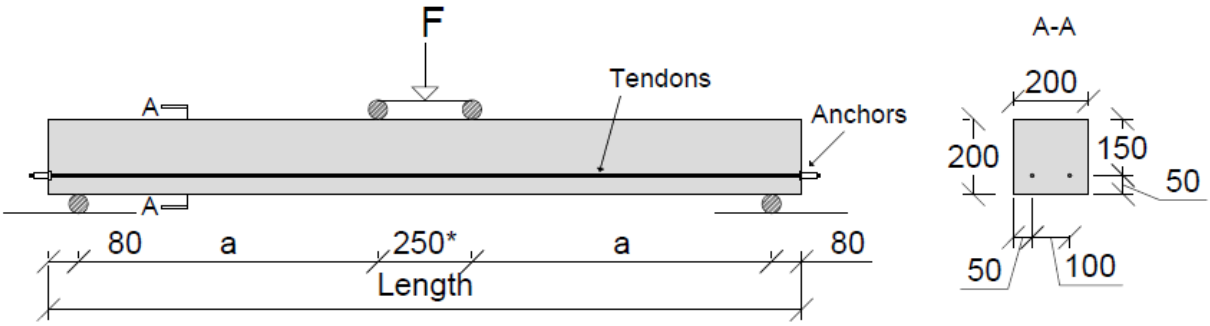

Figure 1. Schematic drawing (not to scale) of the bending test setup and the beams cross section. The parameters Length and a, are listed in Table 1. The depth, d, was in all cases 150 mm. Note, that the span length of the bracket was 500 mm instead of 250 mm for the 3860 mm long beam.

Table 1. Experimental tested beams. Size, properties and results.

Model	length	*a*	*a/d*	f'_c	*P*	A_f	ρ	$V_{exp.}$	*M* at failure	$V_{craking.}$	Δ	ε at top face
	[mm]	[mm]	-	[MPa]	[kN]	[mm^2]	-	[kN]	[kNm]	[kN]	[mm]	‰
3	1200	395	2,63	67,4	84	156	0,0052	77,5	30,6	33	17	3,25
				67,4	84	156	0,0052	72,0	28,4	38	15	2,90
1	2000	795	5,30	60,4	78	156	0,0052	29,5	23,5	16,5	33	-
				60,4	78	156	0,0052	33,5	26,6	17,5	35	-
				60,4	78	156	0,0052	29,0	23,1	16,5	33	2,60
4	2700	1145	7,63	61,7	84	156	0,0052	23,1	26,4	11,5	53	3,13
				61,7	84	156	0,0052	23,2	26,6	11,5	56	3,25
2	3860	1600	10,67	57,1	78	156	0,0052	15,8	25,3	9	124	2,50
				57,1	78	156	0,0052	15,5	24,7	9	117	3,00
		Average		61,5	81				26,1			

Two strain gauges, 30mm in length each, were glued on the compression site (at the top of the section) in the mid-span of the beam. The maximum strains observed are listed in the last column of Table 1. The listed values are in promill (‰). Two extra beams of same size, with length 3860 mm were tested with external stirrups as shown on Figure 2, to prevent diagonal tension shear failure, which was observed for all the other beams.

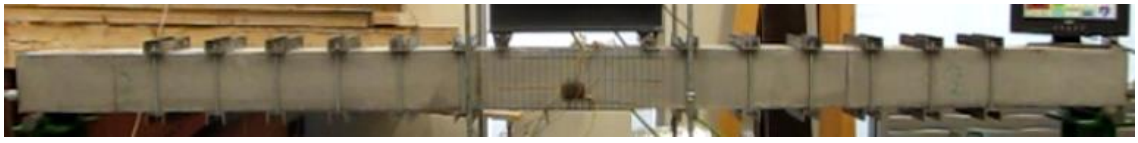

Figure 2. External stirrups on two extra beams of Model type 2, with length of 3860 mm.

Failure mode of the beams prestressed by BFRP tendons was due to bending-shear failure. As shown in Table 1 the failure moment was nearly constant for all of the beams (from 23,1 KNm to 30,6 KNm). The maximum shear force at failure depended on the a/d ratio. This indicates that the a/d ratio has great effect on the shear capacity, although most shear equations published in standards and guidelines do not

consider it directly. For the two beams clamped with external shear links (same size as Model 2), maximum force, **F**, reached 35 and 36,7 KN, see Figure 3, beam 1 and 2. For those beams, the shear at failure reached 17,9 KN instead of 15,7 KN for beams without shear links. These two beams failed on the compression side at the centre of the beam. The maximum bending moment was 28,64 KNm.

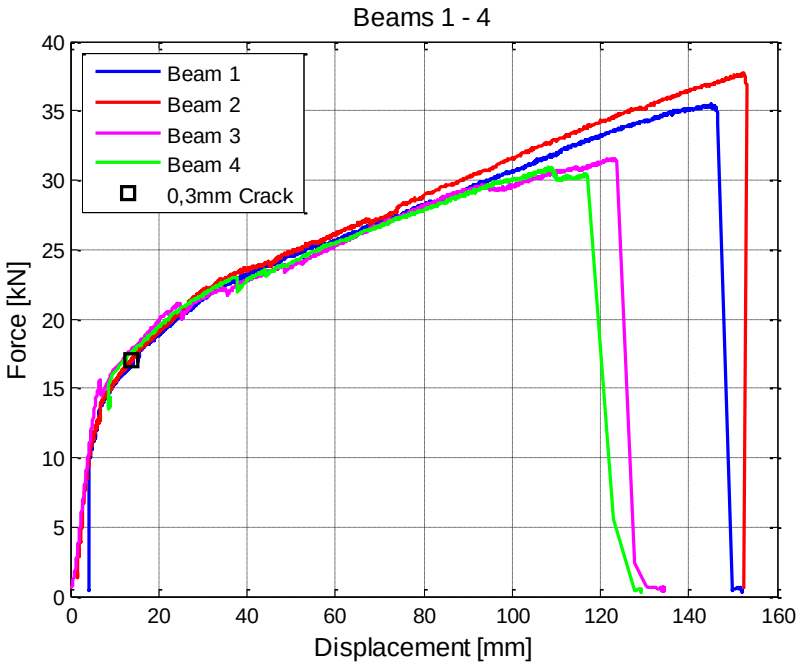

Figure 3. Force displacement relationships for beams 1-4, Beams at length 3860 mm. Beam 1 and 2 are equipped with external shear links, see figure 2.

Monitoring of pre-tensioned BFRP bars to estimate loss of prestress.

The extent of relaxation of tendons used to implement prestress in concrete is a very important factor for designers because it, among other factors, controls the effective prestress force in the concrete (fib , 2007). The ACI sub-committee 440K has for example, developed a test method to estimate long-term relaxation of FRP tendons. The test is usually carried out by stretching a tendon and then holding it at constant temperature for a certain time. From that observation, a relaxation curve over a time interval can be created and the relaxation rate determined as the absolute value of the slope of the curve. The relaxation rate is then used to estimate long-term relaxation (ACI 440R-04, 2004).

There often is a variability in the FRP production, regarding the basic structure as well as amount and type of resin and fibres used. This is unfortunate, because this variation affects the relaxation of the FRP materials. Hence, relaxation varies between types of FRPs and can even vary for the same type of FRPs. Other factors that affect relaxation of FRP materials are the size of the specimen and the tension force applied to the fibres. The ACI sub-committee recommends that the tensile force applied to FRPs be 40-65% of ultimate tensile strength compared to 85% for steel. That, however, does not include BFRP rebars (ACI 440R-04, 2004).

The fib model code 2010 (fib,2012) provides values for relaxation of GFRP, CFRP and AFRP tendons. The 50 years relaxation of GFRP tendons is expected to be in the range of 4,0%-14,0%, for CFRP tendons 2,0-10,0% and for AFRP tendons 11,0-25,0%.

Long-time relaxation testing of BFRP rebars has been ongoing since January 2013 at SEL/RU. Three BFRP 10 mm rebars from MagmaTech Ltd UK were prestressed to 50% of fracture strength. The bars are in an open-air environment at the laboratory shielded by plywood plate formwork. Gunnarsson (2013) published the first measurements. Since then, additional measurements have been taken regularly. The

results are shown in Figure 4. From these measurements, it is estimated that the 50-year relaxation is 6% for the BFRP rebars under investigation.

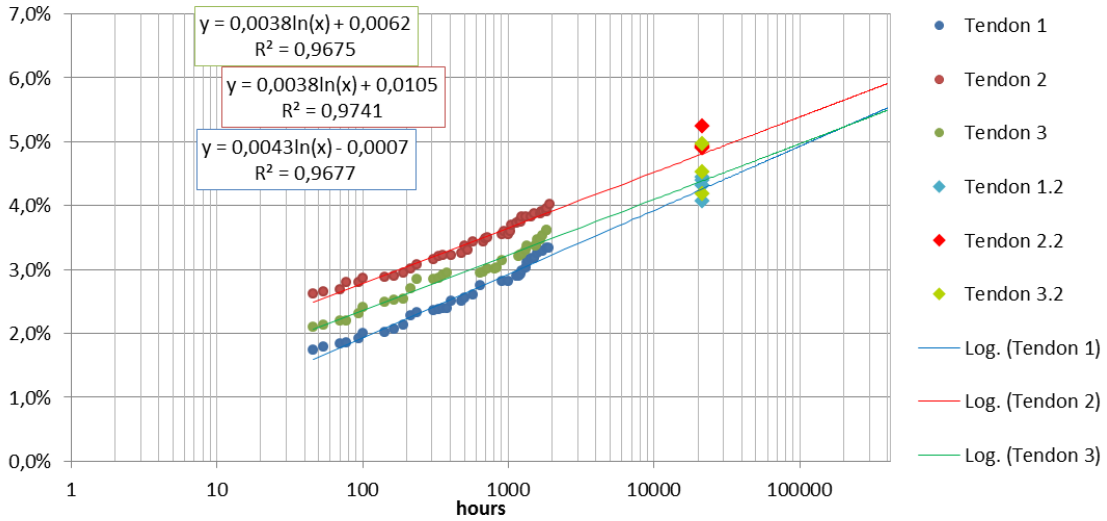

Figure 4. Relaxation of pretensioned BFRP bars.

Concrete panels with basalt fibermats as tension reinforcement.

Thin concrete panels of 20 mm, 35 mm and 50 mm thickness were designed and tested. The reinforcement in the panels was basalt fiber net instead of steel reinforcement. The potential uses of the panels are for precast walls and also as façade elements on in-situ reinforced buildings. The concrete mixture was designed and also the manufacturing process. The panels were tested when they had reached 28-day strength in four-point bending test. The panels show elastic behaviour. The basalt net in the middle of the panels seems to perform as expected (Gíslason, 2015) and is believed to minimize the risk of crack formation.

The strength of the panels was tested at three different cross sections containing a basalt fiber mat. Three different cross-sections were examined. Three samples were made for each cross-section and results of the experiments were obtained by measuring the tensile strength of the samples. The experimental results were then compared with analytical models and the European Standard EN 1992- 1-1. It was found that the strength of the 20mm thick panels was more than twice the strength predicted. The difference was slightly less for the thicker cross-sections. The 35mm cross-section was 68% stronger and the 50mm cross-section was 65% stronger than calculations had indicated.

Measurements of the frost resistance of the concrete mixture also provided positive results. The peeling measured from the concrete mixture was far below the limit values and well below the strict limit.

Overall, the results of this experiment are positive. The cross sections performed well in testing and so did the concrete mixture. Extensive savings in material and cost can be made by reducing the cross section of the traditional weather coating of precast wall elements from 70mm down to 20mm, as corrosion protection is not needed when using FRP materials. Also the weight of the precast units will be less, which will result in reduced transportation costs.

External basalt-mats for columns

Two groups of columns were prepared and tested. (Thorhallsson and Konradson, 2013a) Group CA contained five columns with a corner radius of 20 mm and group CB contained five columns with a corner radius of 35 mm. All columns were the same size of 180 x 180 mm with a length of 1400 mm. All the columns were reinforced in the same way, using one longitudinal bar of diameter 12 mm of steel grade B500C in each corner and hoops of the same steel grade were spaced at 180 mm intervals. Figure 5. The

same size of column specimen was used in previous research at SEL to investigate the ductility of reinforced concrete columns with different hoop spacing. Each group contained a column wrapped with one, two and three layers of BFRP jacket and one column without BFRP jacket as a reference. The basalt mats were from BASALTEX of type BAS UNI 600. The epoxy resin was from Sika.

1C, 2C, 3C and 1M indicates the locations of strain gages.

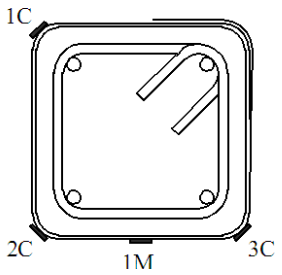

Figure 5: Plain reference column, column with rounded corners and prepared surface, wrapped column in process, BFRP confined column with one, two or three layers. A section cut is shown to the right.

The results are summarized by reporting the key parameters at milestones throughout the loading time in Table 2 and Table 3. Each table includes the unconfined axial load capacity at first peak, Fc, for the unconfined columns, and Fcc_1 for the confined columns; the confined axial load capacity at the jacket rupture Fcc and the load capacity at the failure of the unconfined columns Fcu. Corresponding strain at Fc is ε_{c1}, at Fcu it is ε_{cu}, at Fcc_1 it is ε_{cc1}, and at Fcc it is ε_{cu}. For comparison of the performance of confined columns and the unconfined columns, the strength ratio Fcc1/Fc, Fcc/Fc and the strain ratio ε_{cu} /ε_{c1} is shown. The confinement ratio, MCR defined by Mirmiran et.al, (1998) are listed with number of BFRP layers n.

Table 2. Results of unconfined columns.

Column	n	F_c (kN)	F_{cu} (kN)	ε_{c1} (%)	ε_{cu} (%)
CA0	0	1129,5	1111,1	0,346	0,348
CB0	0	1076,7	1068,5	0,343	0,344

Table 3. Results of confined columns (n=number of layers).

Column	n	MCR	F_{cc1} (kN)	F_{cc} (kN)	F_{cc1}/F_c	F_{cc}/F_c	ε_{cc1} (%)	ε_{cu} (%)	$\varepsilon_{cu}/\varepsilon_{c1}$
CA1	1	0,05	1179,4	971,2	1,04	0,86	0,332	0,783	2,26
CA2	2	0,09	1169,7	1197,6	1,04	1,06	0,270	0,950	2,74
CA3	3	0,14	1310,1	1355,7	1,16	1,20	0,344	1,378	3,98
CA3	3	0,14	1310,1	1520,2	1,16	1,35	0,344	1,088	3,14
CB1	1	0,08	1127,1	1048,3	1,05	0,97	0,330	0,711	2,07
CB1	1	0,08	1127,1	1078,4	1,05	1,00	0,330	0,655	1,91
CB2	2	0,17	1193,2	1497,2	1,11	1,39	0,286	1,014	2,95
CB3	3	0,25	1209,5	1527,3	1,12	1,42	0,332	2,198	6,40

All BFRP confined specimens had similar stress-strain behaviour in the ascending part of loading before the first micro cracks developed since the lateral dilation was very small. This behaviour confirms that the passive confining pressure provided by the BFRP jacket is negligible during the loading state up to the transition zone where micro cracks start to develop.

During the ascending part of loading up to the first peak load, no visual cracks were seen in the concrete cover of the reference columns CA0 and CB0 (columns without basalt strengthening). Right after reaching the peak load (see F_c in Table 2), longitudinal bars buckled between hoops and the concrete separated in an explosive way. Since there was no plastic deformation in the reinforcement, the columns failed in a brittle manner giving no warning of failure. As seen in Table 2 there was very little difference between Fc and Fcu at failure. In both of these columns, the failure occurred at the top of the centre region between the uppermost hoops spaced 180 mm apart.
Increase in compressive strength at first peak was observed in all confined specimens. See F_{cc1}/F_c in Table 3. This is because the BFRP jacket activates in the transition zone where micro cracks developed and is fully activated after reaching the unconfined concrete strength where the cracks developed rapidly. After reaching the load capacity at first peak, all columns except CB3 exhibited a rapid descending slope while the BFRP jacket activated and started to resist the concrete dilation and buckling of the longitudinal bars. With the BFRP jacket fully activated, the load capacity started to increase again in stress-strain behaviour of a hardening response with increase in axial strain. Column CA1 however did not increase its load capacity after the BFRP jacket was fully activated but retained it constant until the jacket ruptured. Instead of a rapid descending slope after first peak, column CB3 kept the axial resistance at peak constant, which then further increased until the jacket ruptured. Columns with increased axial load capacity generally reached a second peak where the maximum confined load capacity was reached and first rupture of fibres occurred. Load capacity at ultimate was where the BFRP jacket failed resulting in failure of the columns.
As the axial deformation and dilation increased, more crack sounds could be heard until the first fibre rupture was observed. Axial strain generally continued to increase with decrease in axial load capacity and buckling of longitudinal bars until next fibres ruptured which resulted in rupture of the jacket. Right before the jacket ruptured, white patches began to show at the rupture location which indicated a plastic flow of the resin. (Figure 6).

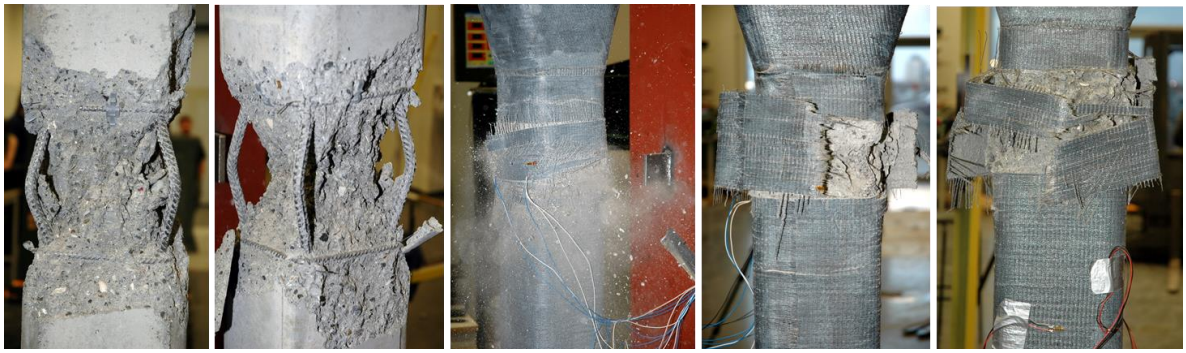

Figure 6: Failure modes: Local buckling of longitudinal bars, symmetric buckling of longitudinal bars, BFRP jacket during failure, BFRP jacket rupture at corner 1C, BFRP jacket failure at corners 2C and 3C.

Fibre rupture generally occurred at the curvature changing point of the corners. Delamination was observed in the overlap on columns CA1 and CB1 before the jacket rupture but did not result in rupture of fibres and therefore had no affect on the confined load capacity. All columns failed at the uppermost hoop space of 180 mm.

Glulam beams strengthened at bottom lamella.

The purpose of the project was to examine the feasibility of strengthening glulam beams by gluing basalt fibres to the tension zone and to investigate if pre-stressing the fibres would increase strength and improve performance. Efforts were made to find a method of pre-stressing the fibres without the need for large equipment and much complexity that is, a method that could even be used at a building site. The fibres were pre-stressed using cambering. The method is based on the beam being cambered with a

single force in the middle to a certain extent before the fibres are glued on. When the cambering force is released, the beam corrects itself and stretches the fibres.

Results from a numerical model considers the linear elastic behaviour and the plastic behaviour of the timber under compression are compared with the results from the mechanical testing of non-strengthened glulam beams and beams strengthened with BFRP and with GFRP. (Thorhallsson, Hinriksson and Snaebjornsson, 2016b)

24 glulam beams (3,2 m long, 65 mm wide and 167 mm high) were tested. Half of the beams were in strength class GL32h and the second half were in strength class GL30c. The basalt fibres used for the glulam beams of strength class GL32h in the experiment are called BAS UD 280.1350.P supplier Basaltex. They are unidirectional mats and the fibres relative density is 280 g/m^2. The basalt fibres used for the glulam beams of strength class GL30c in the experiment are called BAS UNI 350 also from Basaltex. They are also unidirectional mats but the fibres relative density is 416 g/m^2. Both types of basalt fibre mats used, have a fracture strength 2500 MPa, elastic module 84 GPa and max elongation of 3,15 %. The glass fibres used in the experiment are from Saertex and they are E-glass fibres. They are unidirectional mats that weight 912 g/m^2, 0,8 mm thick and elastic module 73 Gpa. The resin used was SP 115 two components epoxy glue from Gurit. Tensile strength according to the manufacturer is 70,3 MPa and modulus of elasticity is 3,67 GPa.

The beams were tested in a four-point bending test. The beams were randomly divided into groups with 3 or 4 beams in each group. For each group the bottom laminate of the beams was reinforced with slack basalt fibres, slack glass fibres, pre-stressed basalt fibres or with no reinforcement for comparison. Reinforcement ratio of BFRP was 0,5% and 0,75% , calculated as the area proportion of fibres mats and resin to the glulam cross-section area. For comparison, seven beams without reinforcement (naked) were tested and also four beams strengthen with GFRP laminate with 0,5% reinforcement ratio.

In Table 4 mean values for each tested category are shown. The error of the model is estimated 0,97-1,20 for the bending strength, modulus of rupture (MOR). And for stiffness, beams modulus of elasticity (MOE), the ratio is 0,92-1,54. The naked beam t13 –t16 gives unexpected high stiffness, that is the reason why the error factor reach 1,54.

Table 4. Comparison of each category with the mathematical model.

			Experiment			Analytical model			Comparison		
			M_{exp}	E_{exp}	ε_{FRPexp}	M_{mod}	E_{mod}	ε_{FRPmod}	$M_{exp}/$	$E_{exp}/$	$\varepsilon_{FRPexp}/$
Beam	Fibre ratio	Glulam	[kNM]	[MPa]	%	[kNM]	[MPa]	%	M_{mod}	E_{mod}	ε_{FRPmod}
t1-t3	Naked beam	GL32h	12,47	15640		12,80	13700		0,97	1,14	
t4-t8	0,5% BFRP	GL32h	17,87	18704	0,32	16,53	18593	0,38	1,08	1,01	0,84
t9-t12	0,5% GFRP	GL32h	19,55	18977	0,29	16,32	17410	0,38	1,20	1,09	0,76
t13-t16	Naked beam	GL30c	11,90	20188		11,90	13150		1,00	1,54	
t17-t20	0,75% BFRP	GL30c	16,30	22359	0,39	15,95	24257	0,37	1,02	0,92	1,05
t21-t24	0,75 % prestress BFRP	GL30c	19,53	24089	0,70	19,71	24257	0,69	0,99	0,99	1,01

All the beams tested, failed at the tension side either due to a knot in the lower edge (tension side) or from shear bending failure in the centre span of the beam. No delamination was noticed between fibres and the glulam beam during the testing. The fibres were undamaged as expected and measured maximum strain in the slack fibres was 0,39% or just only 12% of fracture strain of the BFRP. For the prestress BFRP max strain measured was 0,81% or 25% of maximum BFRP strain.

A noticeable increase in strength can be seen when the average flexural strength of the unreinforced beams is compared with the average flexural strength of the reinforced beams. When the beam is

reinforced with basalt fibre mats or glass fibre mats an increase in strength of 37% - 57% is observed. By using pre-stressing methods 64% higher moment capacity and 19% higher modulus of elasticity can be achieved.

Final remarks

The main conclusion reached through the above listed experimental work, is that BFRP is a promising structural material for various types of civil engineering structures that can complement and/or replace current building materials.

BFRP tendons can replace traditional reinforcing steel if properly implemented. In general however, the shear strength of FRP beams is less than that of steel-reinforced beams as the dowel actions are much lower for the FRP beams. BFRP prestressed beams without shear reinforcement are vulnerable to transverse loading even when the a/d ratio is high. Comparison of the experimental results and relevant shear equations in design guides/standards showed, that both shear force and bending moment distribution along the span of the beams need to be considered to determine the shear capacity.

A relaxation test done on BFRP tendons at the SEL, Reykjavik University estimates an expected final value 6% relaxation of 50 years. This is about the same relaxation as can be expected for glass fibre bars.

The experimental testing of confined reinforced concrete columns clearly demonstrated that BFRP wrapping can enhance the structural performance of concrete columns under axial loading. The confinement effect is directly related to the shape of the cross-section. The number of BFRP layers and the corner radius are the major parameters controlling the behaviour of the wrapped concrete columns. These parameters are expressed in the MCR confinement ratio. To enhance the confined behaviour, the stiffness of the BFRP jacket can be increased by applying additional layers as well as by increasing the corner radius of square columns.

The production and testing of the thin sandwich panels, reinforced with basalt fiber net, showed that this innovation is an interesting option for the precast building industry. With this new design, it is possible to manufacture thin external facades and reduce both weight and $C0_2$ emissions.

It is found that a significant improvement is achieved by reinforcing glulam beams with slack and pre-stressed basalt fibres. A noticeable increase in average flexural strength compared to unreinforced beams. The experiments also showed that a more ductile behaviour is achieved for the composite beam, as the FRP material is in the working stress range when the timber ruptures and the beam will not totally collapse as the FRP material holds the glulam boards together at the tension side.

Acknowledgements

The authors greatly appreciate the financial support from NordMin and Rannis and support from the Innovation Center Iceland, Limtré Vírnet ehf (Iceland) and Professor Olafur Wallevik. The work done on this topic by Bjorgvin Smari Jonsson, Sindri Gudmundsson, Arngrimur Konradsson, Andri Gunnarsson, Guðmundur Úlfar Gíslason, Ívar Hauksson, Guðjón Rafnsson and Guðmundur Hinriksson a research students at Reykjavik University is acknowledged.

References

ACI 440R-04. (2004). Prestressing concrete structures with FRP tendons. Farmington Hills, MI: American Concrete Institute.

fib. (2007). FRP reinforcement in RC structures.Bulletin No. 40. Lausanne, Switzerland.: fédération internationale du béton (fib).

fib. (2012). Model Code 2010 - Final draft, Volume 1, Bulletin 66. Lausanne, Switzerland: fédération internationale du béton (fib).

Gíslason, Guðmundur Úlfar. (2015) Concrete sandwich panels with BFRP reinforcement. (B.Sc. thesis). Reykjavik University.

Gunnarsson, Andri (2013). Bearing capacity, relaxation and finite element simulation for prestressed concrete beams reinforced with BFRP tendons (M.Sc. thesis). Reykjavik University.

Johannesson, Birgir, Thorsteinn Ingi Sigfusson, Hjalti Franzson, Ögmundur Erlendsson, Björn S. Harðarson, Eythor Rafn Thorhallsson, Arni B. Arnason, Kamal Azrague, Marianne Rose Kjendseth Wiik, Sirje Vares, Anna Kronlöf, Pertti Koskinen, Tapio Vehmas (2017): *GREENBAS Sustainable Fibres from Basalt Mining*. Edited by Birgir Johannesson; Nordic Council of Ministers., ISBN: ISBN 978-92-893-4809-6, DOI:10.6027/TN2016-564

Mirmiran, A., M. Shahawy, M. Samaan, H. E. Echary, J. C. Mastrapa and O. Pico. (1998) Effect of column parameters on FRP-confined concrete. Journal of Composites for Construction, vol. 2, pp. 175-185.

Thorhallsson, Eythor Rafn, Jónas Thór Snaebjornsson (2016a): Basalt Fibers as New Material for Reinforcement and Confinement of Concrete. Solid State Phenomena; 249:79-84., DOI:10.4028/www.scientific.net/SSP.249.79

Thorhallsson, Eythor Rafn, Gudmundur Ingi Hinriksson, Jonas Thor Snæbjornsson (2016b): Strength and stiffness of glulam beams reinforced with glass and basalt fibres. Composites Part B Engineering 10/2016; DOI:10.1016/j.compositesb.2016.09.074

Thorhallsson, Eythor; Todor Zhelyazov, Andri Gunnarsson, Jonas Thor Snaebjornsson (2015): *CONCRETE BEAMS REINFORCED WITH PRESTRESSED BASALT BARS*. Concrete-Innovation and Design, fib Symposium, Copenhagen, Denmark

Thorhallsson, Eythor; Andri Gunnarsson, Jonas Thor Snaebjornsson (2014a): *SIMULATION OF EXPERIMENTAL RESEARCH OF CONCRETE BEAMS PRESTRESSED WITH BFRP TENDONS*. Nordic Concrete Research Symposium, Reykjavik, Iceland

Thorhallsson, Eythor; Jon Olafur Erlendsson, Guðmundur T Bergsson (2014b): *Composite lighting poles from basalt fibers*. 1st International Conference on Mechanics of Composites, Stony Brook University, Long Island, USA

Thohallsson, Eythor; Arngrimur Konradsson (2013a): Renovation of Concrete Columns by Wrapping Basalt Fiber Sheets. 05/2013; 99(18)., DOI:10.2749/222137813806501452

Thorhallsson, Eythor; Jón Ólafur Erlendsson, Ögmundur Erlendsson (2013b): *Basalt fiber introduction*. NordMin Information Day and Brokerage Event, Copenhagen.

Thorhallsson, Eythor; Sindri Hlifar Gudmundsson: *Test of prestressed basalt FRP concrete beams with and without external stirrups*. (2013c) In proceedings of Fib symposium Engineering a Concrete future: Technology, modelling & Construction, Tel Aviv. Israel

Thorhallsson, Eythor; Bjorgvin Smari Jonsson (2012): *TEST OF PRESTRESSED CONCRETE BEAMS WITH BFRP TENDONS*. Workshop Structural Engineering and Composites Laboratory, Reykjavik Univeristy, Reykjavik, Iceland

Thorhallsson, Eythor; Arngrimur Konradsson, Stefan Kubens (2011): *Strengthening of concrete columns by wrapping basalt fiber matrix*. . Nordic Concrete Research Symposium 2011, Hämeenliina, Finland.

Wiik, Marianne Kjendseth; Eythor Thorhallsson, Kamal Azrague: (2017) A mechanical and environmental assessment and comparison of basalt fibre reinforced polymer (BFRP) rebar and steel rebar in concrete beams. Energy Procedia 01/2017; 111(C):31-40., DOI:10.1016/j.egypro.2017.03.005

Williams, Steven E. (2015) : FRP Rebar in Slabs on Grade Benefit from Low Modulus of Elasticity. http://neuvokascorp.com